Understanding the Subseasonal Modulation of Moisture Transport over the Indian Monsoon Domain.

J. M. Neena[1], Dilip. V[1]., and Aneesh C. Subramanian[2]

[1]Earth and Climate Science,
Indian Institute of Science Education and Research Pune, India.

[2]Department of Atmospheric and Oceanic Sciences,
University of Colorado Boulder, Boulder, CO, USA.

Corresponding author
J. M. Neena,
Earth and Climate Science,
Indian Institute of Science Education and Research Pune,
Dr Homi Bhaba Road, Pashan, Pune,
Maharashtra, India.
E-Mail: neena@iiserpune.ac.in
Phone: +91-02025908182

Abstract

The subseasonal modes of integrated water vapor transport (IVT) over the Indian Summer Monsoon (ISM) domain were examined and their association with different modes of ISM precipitation was analyzed during boreal summer seasons from 1979-2018. The IVT over the monsoon domain was found to exhibit significant variability in the intraseasonal (20-60 days), quasi-biweekly (10-20 days), and synoptic (3-10 days) time scales. The intraseasonal IVT mode is dominant between 0-20°N and reflects the fluctuations of the low-level jet stream. The quasi-biweekly and synoptic-scale IVT variability dominates over the Bay of Bengal and the Indo-Gangetic plain. The intraseasonal IVT mode is the most dominant and it is found to influence the higher frequency subseasonal IVT modes. Meanwhile, large-scale factors such as the El Niño Southern Oscillation (ENSO) and the Indian Ocean Dipole (IOD) were found to modulate the intraseasonal IVT mode and negatively impact the monsoon. Lead-lag correlation analysis between the subseasonal precipitation and IVT modes suggests that the IVT anomalies are driven by the subseasonal convective anomalies and associated changes in atmospheric circulation. Since moisture supply from adjoining oceanic regions is fundamental for monsoon precipitation, there is a general tendency to attribute the variability/trends in precipitation to changes in moisture transport. Our analysis of the subseasonal modes of IVT indicates that such inferences may be misrepresentative, as the monsoon diabatic heating in itself is a strong driver of monsoon circulation and moisture transport.

1. Introduction

The strong cross-equatorial monsoon winds combined with the evaporative fluxes from the Indian Ocean, Arabian Sea (AS), and the Bay of Bengal (BoB) contribute to the integrated water vapor transport (IVT) to the Indian summer monsoon (ISM) domain. The equatorial Indian Ocean and the AS are considered as the major sources of moisture for ISM rainfall [Cadet and Reverdin, 1981; Cadet and Greco, 1987; Murakami et al., 1984; Webster and Fasullo, 2003; Levine and Turner, 2012]. Regional moisture budget analysis reveals that different parts of the ISM domain receive moisture fluxes from different parts of the Indian Ocean, AS and BoB, along with significant contributions from local moisture recycling from terrestrial sources [Gimeno et al., 2010; Ordonez et al., 2012; Mie et al., 2015; Pathak et al., 2017a]. The summer mean moisture transport is known to take two major pathways over the ISM domain [Findlater, 1971] - the AS branch transporting moisture from the equatorial Indian ocean, along with evaporative fluxes from AS and the BoB branch transporting fluxes from BoB and central equatorial Indian Ocean. The moisture transported by the AS branch makes a relatively large contribution to the rainfall along the west coast of India, whereas, the precipitation over eastern and north-eastern parts of India is linked to the moisture transported by the BoB branch [Konwar et al., 2012; Gimeno et al., 2010].

Several studies have explored the long-term trends in moisture transport and monsoon rainfall [Konwar et al., 2012; Patil et al., 2016; Ratna et al., 2016]. The seasonal mean IVT and ISM rainfall are found to exhibit similar trends on interannual time scales. Few studies have also explored the moisture transport-monsoon rainfall relationship in the context of intense moisture transport events analogous to “atmospheric rivers” in the mid-latitude regions [Ratna et al., 2016; Patil et al., 2019; Lakshmi et al., 2019]. Moisture transport by atmospheric rivers from tropics to mid-latitudes has been shown to lead precipitation/snowfall events [Guan et al., 2012; Waliser and Guan, 2017]. While some

86 studies have attempted to understand moisture transport associated with high-intensity
87 precipitation events over the ISM domain using the same concept, the prevailing wind
88 patterns and the dominant subseasonal modes of monsoon variability makes the picture much
89 more complicated. Also, due to the strong convection-circulation coupling over the monsoon
90 domain, diabatic heating associated with convection plays a major role in driving the large-
91 scale circulation [Webster and Fasullo, 2003; Jones and Carvalho, 2002; Liebmann et al.,
92 2004] and it is difficult to separate out a predictor-predictand relationship between moisture
93 transport and precipitation.

94 It is well known that the boreal summer monsoon intraseasonal oscillations (MISOs)
95 exert a large control on the amplitude of the seasonal mean ISM rainfall and its interannual
96 variability by controlling the strength and duration of the active-break episodes of monsoon
97 [Lawrence and Webster, 2001; Goswami and Ajayamohan, 2001; Suhas et al., 2012]. The
98 MISOs are the northward propagating counterpart of the Madden Julian Oscillations (MJO)
99 during boreal summer and their signal is evident in several dynamic and thermodynamic
100 fields over the monsoon domain [Goswami, 2005 and references therein]. A quasi-biweekly
101 scale (10-20 day) oscillation is also dominant over the monsoon domain, associated with
102 westward propagation of convective anomalies [Krishnamurti and Ardanuy, 1980; Chen and
103 Chen, 1993; Chatterjee and Goswami, 2004; Kikuchi and Wang, 2010; Ortega et al., 2016].
104 Synoptic scale convective activity in the form of lows and depressions form over BoB and
105 they also contribute significantly to the seasonal mean monsoon [Goswami et al., 2003;
106 Praveen et al., 2015]. Since the seasonal mean ISM rainfall bears a strong relationship with
107 the seasonal mean moisture transport by the monsoon winds, we expect that the IVT-rainfall
108 relationship might also hold in the subseasonal time scales. However, there have been
109 relatively few studies that explored the subseasonal variability of moisture transport. Yoon
110 and Chen [2005] examined the regional water vapor budget over the ISM domain and

111 reported that water vapor convergence into the monsoon trough zone is strongly modulated
112 by the 30–60 day mode. A similar but weaker impact was associated with the 10-20 day
113 mode. Pathak et al. [2017b] reasoned that an active or break phase of ISM is largely
114 determined by whether the moisture convergence happens over the monsoon trough zone,
115 northeast of India or the equatorial Indian Ocean and the relative contributions of moisture
116 fluxes from different oceanic/terrestrial sources are different for the extreme MISO phases.
117 Ordonez et al. [2013] examined the impact of MJO on the water vapor budget associated with
118 the monsoon Low-level Jetstream (LLJ) and the variation in rainfall over India using a
119 Lagrangian model. The MJO modulation of water vapor transport by the LLJ was found to
120 have a significant impact on the rainfall over the monsoon zone. Patil et al. [2019] briefly
121 examined the common periodicities in the IVT and rainfall during contrasting monsoon years
122 and noted the dominance of the 10-20 day mode during strong monsoon years. Nevertheless,
123 a clear picture of the subseasonal modes of moisture transport over the ISM domain has so
124 far been elusive.

125 In addition to predicting the seasonal mean monsoon, efforts are also directed towards
126 predicting the active/break episodes of precipitation which is critical for agricultural practice.
127 While efforts are still underway in expounding the processes and mechanisms driving the
128 MISOs in convection [Jiang et al., 2004; Bellon and Sobel 2008; Dixit and Srinivasan 2011],
129 exploring and understanding the form of relationship between regional circulation and
130 monsoon rainfall, which determines the moisture transport in the intraseasonal time scales,
131 will be of great value. In this study, we try to understand the subseasonal variability in IVT
132 over the ISM domain and explore its potential relationship with convective activity. Large-
133 scale ocean-atmosphere coupled modes like the El Niño Southern Oscillation (ENSO) and
134 the Indian Ocean Dipole (IOD) are known to impact the convergence/divergence pattern over
135 the equatorial Indian Ocean and are also known to impact the MISO [Webster et al. 1998,

Behera and Ratnam 2018]. Hence, we also examine the influences of these phenomena on the subseasonal variability of IVT.

The data and details of the methodology are provided in section 2. Identification of the subseasonal IVT modes, their characteristics, and the relationship with the subseasonal rainfall variability over the region are described in the results and discussion section. The MISO control on the higher frequency IVT modes and the large-scale factors impacting the IVT modes is also presented. The main results and inferences are summarized in the summary and conclusions.

2. Data Methodology

The analyses were performed using ERA-Interim daily reanalysis data [Dee et al., 2011] of horizontal resolution 2.5° from 1000 hPa to 500 hPa for the 1979-2018 period over the monsoon domain (10°S-30°N, 40°E-110°E). Zonal and meridional wind components and specific humidity were used for computing the IVT. Daily IVT values into and out of the monsoon domain were calculated following Fasullo and Webster [2003].

$$IVT = \frac{1}{g}\int_{1000}^{500} (u\,q + vq)\,dp$$

Where u and v are the horizontal wind components, g is the acceleration due to gravity and q is the specific humidity. Integration was performed between pressure levels 1000 hPa and 500 hPa. Daily anomaly fields were calculated by removing the climatological annual cycle from the respective fields. For analyzing the relationship between subseasonal IVT and precipitation, daily TRMM 3B42 (V7) precipitation data [Huffman et al., 2007] from 1998-2018 was used. Representative indices of ENSO (Nino3.4 index), and IOD (Dipole Mode Index (DMI) index) were created by area averaging the sea surface temperature (SST) over the equatorial Pacific Ocean and Indian Ocean respectively [Trenberth, 1997 and Saji et al., 1999]. The DMI index [Saji et al., 1999] is defined as the SST difference between the

159 western (50°E-70°E, 10°S-10°N) and the south-eastern Indian Ocean (90°E-110°E, 0°-10°S).
160 Extended reconstructed sea surface temperature (ERSST) version 4 [Huang et al., 2015] were
161 used for constructing the indices. We have also used an alternate index for IOD, the
162 EQUINOO index, which represents the atmospheric component of the coupled IOD mode
163 [Gadgil et al. 2004]. EQUINOO index is the negative of the zonal wind at 850 hPa averaged
164 over the region 60°E-90°E, 2.5°S-2.5°N. The El Niño/La Niña years were identified as when
165 the boreal summer mean Nino3.4 Index exceeded a threshold of +/- 0.5°C respectively. IOD
166 positive and negative years were identified as when the boreal summer mean EQUINOO
167 index exceeded a threshold of +/-0.5, respectively (Table 1).

168 **3. Results and Discussions.**

169 **3.1 The Subseasonal IVT modes**

170 The dominant subseasonal modes of IVT during June to September monsoon season
171 is studied using empirical orthogonal function (EOF) analysis of daily IVT anomalies from
172 1979-2018 (Figure 1). The conventional approach for studying IVT variability focuses on the
173 monsoon LLJ and area averages of IVT over AS and BoB domains. Since the LLJ exhibits
174 significant interannual variability in its position and strength [Sandeep and Ajaymohan 2015;
175 Varikoden et al., 2018], we have refrained from using fixed geographical boundaries for
176 defining AS or BoB moisture transport. The EOF analysis was carried over the ISM domain
177 from 10°S to 30° N, 40°E to 110°E. The first two EOF modes (Figure 1 a & b) together
178 explain about 33 % of the seasonal IVT variance and it represents the two preferred phases of
179 moisture transport by the LLJ, across the equatorial Indian Ocean and across the southern
180 peninsular region of India. Power spectral analysis of the principal components (PC)
181 corresponding to these two modes (Figure 1 e & f) show that these modes of IVT are
182 associated with variability in the 20-60 day timescale with spectral peaks at these time
183 periods. Unlike the first two modes, the third and fourth EOF modes (Figure 1 c & d) show

184 an east-west loading of variances capturing the moisture transport over AS and the BoB. The
185 PC power spectra (Figure 1 g & h) indicate that these modes represent variability in the
186 quasi-biweekly and synoptic time scales. Unlike the intraseasonal and quasi-biweekly modes,
187 the synoptic-scale separation by EOF analysis is not very clean as it includes a portion of the
188 quasi-biweekly scale as well. In short, using EOF analysis we are able to separate out the
189 dominant spatial and temporal scales of IVT over the ISM domain.

190 The low-frequency intraseasonal scale, quasi-biweekly scale and synoptic-scale IVT
191 modes were extracted by applying 20-60 day, 10-20 day and 3-10 day bandpass filter to the
192 daily IVT values. Examination of the IVT variance in these timescales indicate that the
193 domain of activity of each of the three modes are different (Figure 2), suggesting that the
194 different scales of IVT variability might have regional preferences. Synoptic scale IVT
195 variability (Figure 2a) is dominant over the head bay and the foothills of the Himalayas. The
196 quasi-biweekly IVT variance (Figure 2b) exhibits a pattern similar to the synoptic scale,
197 while the largest amplitude is observed over BoB. The 20-60 day intraseasonal IVT variance
198 (Figure 2c) has the largest amplitude over the region of LLJ activity. Notably, the
199 intraseasonal IVT variance is dominant to the south of 20°N, and relative to the
200 synoptic/quasi-biweekly timescales, the intraseasonal variance is weaker over the Indo-
201 Gangetic plain. The dominance of synoptic to quasi-biweekly scale IVT variability over the
202 Indo-Gangetic plain may be related to the fact that the passage of synoptic-scale lows and
203 depressions majorly contributes to the rainfall variability over the region [Goswami et al.,
204 2003; Praveen et al., 2015].

205 Month to month changes in the amplitude of the three subseasonal modes were further
206 examined (Figures 3, 4 and 5) to understand the IVT variability during the onset and mature
207 stages of monsoon. The IVT variance associated with the three modes were examined for
208 individual months from May to October. While the synoptic-scale IVT variance is relatively

small in May, over the head bay region, it strengthens in June, with the domain extending northwestward into central India (Figures 3 a & b). During June, significant synoptic-scale IVT variability is also observed over the eastern AS and west coast of India. Peak synoptic-scale IVT variance is observed during July and August months (Figures 3 c & d). The region of significant synoptic-scale IVT variability is now spread over a larger domain covering the Indo-Gangetic plain and Bay of Bengal. Maximum variance is observed over the head bay and the foothills of Himalayas. The synoptic-scale IVT variance decreases in September and October, following the monsoon seasonal cycle (Figures 3 e & f). Like the synoptic scale mode, the quasi-biweekly scale IVT variance is also concentrated over BoB, but the center of maximum variance is observed to the south of the head bay (Figure 4). During June, significant quasi-biweekly scale IVT variability is also observed over the eastern Arabian Sea (Figure 4b) pointing towards the possible association of quasi-biweekly scale IVT variability with the monsoon onset. June and July mark the months of maximum quasi-biweekly scale IVT variability, when significant IVT variance is observed to extend over land, from peninsular to northern India (Figure 4 c & d). It weakens from August to October. The intraseasonal variability of IVT in the 20-60 day timescale follows the variability in the strength and location of the LLJ (Figure 5). While the 20-60 day IVT variability is confined to the eastern equatorial Indian Ocean and BoB during May (Figure 5 a), as the monsoon develops, during June and July, strong intraseasonal IVT variability is observed between 10°N to 20°N. The IVT variance is equally strong over AS and BoB during June (Figure 5 b), but during July and August the variance maxima are shifted eastward over BoB (Figure 5 c & d).

3.2 Subseasonal IVT-precipitation relationship

IVT analysis is often motivated by the presumption that moisture transport leads to precipitation. Some recent studies have attributed the observed trends in seasonal mean ISM

234 rainfall with the trends in IVT [Konwar et al., 2012; Ratna et al., 2016]. High intensity
235 localized monsoon precipitation events and associated floods are connected to high amplitude
236 IVT events across the AS and BoB [Patil et al., 2019; Lakshmi et al., 2019], and biases in
237 simulating the monsoon rainfall patterns by climate models are attributed to the limitations in
238 the models in accurately simulating the moisture transport patterns [Levine and Turner, 2012;
239 Sahana et al., 2019]. While there is no contestation to the fact that large-scale precipitation
240 and moisture transport are fundamentally linked in a coupled system such as the monsoons, it
241 will be problematic to make such broad attributions without understanding convection-
242 moisture influx relationships at different timescales. Hence, we explored the nature and form
243 of relationship between monsoon precipitation and IVT on the subseasonal timescales.

244 The intraseasonal, quasi-biweekly and synoptic-scale modes of monsoon precipitation
245 were extracted by applying a 25-60 day, 10-20 day and 3-10 day bandpass filter to the
246 precipitation anomalies over the ISM domain during the 1998-2018 June to September
247 monsoon season. A lead-lag correlation analysis between IVT and precipitation variability
248 was carried out to understand whether the two variables coevolve simultaneously or evolve
249 with a finite phase difference. The principal component of the first EOF mode (PC1) was
250 considered as the reference time series for the 20-60 day intraseasonal IVT variability and it
251 was correlated with 25 - 60 days filtered precipitation time series at every grid point over the
252 ISM domain at different lags from -12 day to +12 day (Figure 6). While both PC1 and PC2
253 capture the intraseasonal IVT variability, we chose PC1 as the reference time series since it
254 corresponds to the positive phase of IVT activity over the subcontinent. A positive lag means
255 that precipitation lags IVT. The large-scale structure of the MISO is evident from the
256 northwest-southeast tilted structure of positive correlations extending from northwest India to
257 equatorial west Pacific. The lag-correlation maps bring out coherent variations in
258 precipitation and IVT in the intraseasonal timescales as the band of positive correlations

follow the northward excursion of MISO from the equatorial Indian Ocean to the foothills of Himalayas. Maximum positive correlations are observed at lag 0, lag 3 and lag 6 days, when IVT lags rainfall. On the other hand, when intraseasonal precipitation variability lags the IVT variability (positive lags), the positive correlations are rather weak. The analysis indicates that the IVT variability in the 20-60 day timescale may be driven by the diabatic heating associated with intraseasonal precipitation variability, which corroborates previous studies [e.g., Joseph and Sijikumar, 2004; Annamalai and Sperber, 2005] who showed that the intraseasonal variations of the LLJ are mostly driven by intraseasonal convective activity.

A similar analysis was performed using PC3 as the reference time series for the 10-20 day quasi-biweekly IVT mode and correlating it with 10-20 day filtered precipitation anomalies at different lags from -6 day to +6 day (Figure 7). The lag correlation maps bring out a northwestward propagation of positive correlations from the South China Sea to northwest India. It is well known that the quasi-biweekly scale variability of monsoon is associated with northwestward propagating convective disturbances from the west Pacific to the ISM domain [Krishnamurti and Ardanuy, 1980; Chatterjee and Goswami, 2004; Kikuchi and Wang 2010]. The quasi-biweekly scale precipitation variability over central BoB shows a maximum positive correlation with the quasi-biweekly scale IVT variability at a lag of 4 and 6 days, indicating that, similar to the MISO scale, convective activity in the quasi-biweekly scale might be a major driver for the moisture transport. Meanwhile, over the eastern AS and over the head bay, maximum positive correlation is observed at lag 0 and a lead of +2 days, indicating that the IVT- precipitation relationship is more or less in phase over these regions.

The relationship between the synoptic-scale IVT variability with precipitation was examined by using PC4 as the reference time series and correlating it with 3-10 day filtered precipitation anomalies at each grid point, from lag 4 days to lead 4 days (Figure 8). Even though the PC4 power spectra indicates some power in the quasi-biweekly timescale also,

extending to about 15 days, we use it to represent the synoptic scale variability as the dominant peak in power is observed for less than 10 days time period. Similar to the quasi-biweekly scale, the northwestward propagation of synoptic-scale disturbances is evident in the correlation maps. The smaller spatial scale associated with the synoptic scale can be made out by comparing Figures 7 and 8. Again, the maximum positive correlation between precipitation and IVT in the synoptic-scale is observed when precipitation leads IVT (lag -2, -1 days). Another interesting aspect is that the co-variability of precipitation and IVT is limited to the west of 100°E, over the Indian ocean domain. This is a distinct feature, different from the quasi-biweekly scale (Figure 7). It means that the synoptic-scale IVT variability is driven by convective disturbances (lows and depressions) originating over the eastern equatorial Indian Ocean or the BoB, while the quasi-biweekly scale IVT variability is driven by westward propagating disturbances of more remote origin, over the South China sea.

The lag correlation analysis indicates that the three subseasonal modes of IVT variability lag the precipitation variability in these scales. While this excludes the potential use of IVT variability in predicting subseasonal convective activity, understanding the pathways of IVT in different timescales might be useful for predicting the evolution of moisture influx into the monsoon domain. Of the three subseasonal modes, the 20-60 day intraseasonal mode is the most dominant and it coherently evolves with the northward propagating MISO convection. Ordonez et al. [2013], examined the freshwater flux anomalies composited for the MJO phases in summer and inferred that the MJO modulates the precipitation and IVT, predominantly to the south of the central Indian monsoon zone, and such a relationship does not exist over northern India. We assume that such an inference was possibly influenced by the inability of the Real-time Multivariate MJO (RMM) indices in capturing the northward excursion of MJO/MISO over the ISM domain [Suhas et al., 2013].

To better understand the intraseasonal evolution of IVT over the ISM domain, we recreated the different phases of IVT evolution using the normalized PC1 and PC2. Six phases were constructed based on the phase difference between PC1 and PC2. The daily IVT anomalies composited for the six phases, when the total amplitude was greater than one is shown in Figure 9. Phase 1 and 2 correspond to positive IVT anomalies over the equatorial Indian ocean, associated with the equatorial position of the LLJ. During phase 3 and 4, the LLJ moves northward to peninsular India and increases in strength, following the northward migration of MISO. In phase 5, the positive IVT anomalies have shifted further northward to between 15°N - 25°N, and in Phase 6 it weakens over the subcontinent.

We further examined how the intraseasonal precipitation anomalies vary in accordance with the six IVT phases. Daily precipitation anomalies over the ISM domain were composited for the six intraseasonal IVT phases (Figure not shown). The phase evolution of intraseasonal precipitation and IVT anomalies over the subcontinent and over the equatorial Indian ocean during the six IVT phases are depicted in Figure 10. Since intraseasonal convection propagates more northward than intraseasonal IVT, to represent the evolution of intraseasonal precipitation over the subcontinent we area-averaged the precipitation anomalies over the BoB box 17°-21°N, 80°-90°E and the IVT anomalies were averaged over 13°-17°N, 80°-90°E. To represent the evolution of intraseasonal precipitation and IVT anomalies over the equatorial Indian ocean, we area averaged the anomalies over 5°S-0, 80°-90°E. The intraseasonal IVT anomalies are positive over the Indian subcontinent during phases 3, 4 and 5, and it is negative during phases 6, 1 and 2 (Figure 9). On the other hand, the intraseasonal precipitation anomalies are roughly out of phase with the IVT anomalies both over the subcontinent and over equatorial Indian ocean (Figure 10). Over the north box, the IVT anomalies are positive around phase 1, when the precipitation anomalies are negative and the IVT anomalies are negative around phase 4, when the precipitation anomalies are

positive (Figure 10a). Opposite conditions prevail over the south box and a similar antiphase evolution is observed (Figure 10b).

Since the 20-60 day mode is the most dominant timescale in monsoon convection and IVT, we explored whether the intraseasonal IVT plays a role in modulating the higher frequency (quasi-biweekly and synoptic-scale) moisture transport. Using normalized PC3 and PC4 time series, the frequency of occurrence of days of strong quasi-biweekly scale IVT and synoptic-scale IVT, were calculated for each of the intraseasonal IVT phases (Figure 11 a & b). It is evident from the frequency distribution that when the intraseasonal IVT phase is active over the subcontinent (phases 3, 4 and 5), it favors more IVT activity in the quasi biweekly and synoptic scales. This phase preference is further brought out in the composites of 10-20 day and 3-10 day filtered IVT anomalies for positive (phases 3, 4 and 5) (Figure 10 c & e) and negative (phases 1, 2 and 6) (Figure 10 d &f) intraseasonal IVT phases over the subcontinent. The quasi-biweekly and synoptic-scale IVT amplitude is significantly greater when the intraseasonal IVT is active over the subcontinent, compared to when the intraseasonal IVT is active over the equatorial Indian ocean. Reading it together with the antiphase relationship between intraseasonal IVT and precipitation, it can be interpreted that MISO convection over the equatorial Indian Ocean favors a greater number of quasi-biweekly scale and synoptic-scale IVT activity, as compared to when the MISO convection is over the northern location of the monsoon trough.

3.3 Large-scale influences on IVT variability

In the interannual timescale, large-scale climate modes such as the ENSO and the IOD influence the monsoon circulation and also affect the SST anomalies over the Indian Ocean [Webster and Yang, 1992; Webster et al., 1998; Gadgil et al., 2004; Ashok et al., 2001; Behera and Ratnam, 2018]. While the negative phase relation between seasonal mean ISM rainfall and ENSO is well established [Webster et al. 1998], the IOD-ISM rainfall

relationship also depends on the phase of ENSO [Ashok et al., 2001, Behera and Ratnam 2018]. The impact of these large-scale modes on the IVT over the monsoon domain was examined by correlating the ENSO and IOD indices with boreal summer mean IVT at every grid point over the monsoon domain. Figure 12a shows the correlation between seasonal mean IVT over the ISM domain with the Nino 3.4 index. It is clear that the IVT anomalies over the north equatorial Indian Ocean exhibit a significant relationship with the ENSO. The negative correlation centered over the central and eastern equatorial Indian Ocean, implies that an El Niño condition would be associated with reduced IVT anomalies over the region. The negative IVT anomalies may be interpreted as a resultant of the changes in the westerlies over the region forced by changes in Walker circulation [Lau and Wu 2001].

The correlation pattern in Figure 12a however bears a close similarity to the second EOF mode of IVT (Figure 1), and also to the intraseasonal IVT phases 1 and 2 (Figure 9), indicating that the ENSO might be having a stronger influence on the 20-60 day intraseasonal IVT mode. We explored this further by examining the occurrence of intraseasonal IVT phases during El Niño and La Niña years. Nine El Niño years and seven La Niña years were identified between 1979-2018 (Table1). During each May to October season, for the El Niño and La Niña years, the fractional number of days were estimated when the intraseasonal IVT amplitude was greater than one and the intraseasonal IVT phase was active over the Indian subcontinent (Phases 3, 4 and 5) and when the intraseasonal IVT phase was active over equatorial Indian Ocean (Phases 6, 1 and 2) (Figure 9). During La Niña years, 30% days of the season corresponded to intraseasonal IVT phase active over the equatorial Indian Ocean, while only 21% days corresponded to intraseasonal IVT phase active over the subcontinent (Figure 12b). On the other hand, for El Niño conditions the intraseasonal IVT was preferentially more active over the subcontinent (27% days) as compared to the equatorial Indian Ocean (21% days). As we have already observed (Figure 10), intraseasonal convective

activity is roughly out of phase with the IVT activity. So, during La Niña states, when the intraseasonal IVT is preferentially more active over the equatorial Indian Ocean, the intraseasonal convective activity would be more active over the Indian subcontinent. Alternately during El Niño conditions, the intraseasonal IVT would be more active over the subcontinent, and the convective activity would be concentrated over the equatorial Indian Ocean.

The influence of IOD on IVT was examined by correlating the EQUINOO index with the seasonal mean IVT (Figure 12c). We choose the EQUINOO index over the DMI index to examine the relationship between IOD and IVT, since the wind-based EQUINOO index represents the atmospheric counterpart of the coupled IOD mode and exhibits a relatively stronger relationship with ISM rainfall [Gadgil et al. 2004]. The EQUINOO index bears a strong positive correlation (correlation coefficient 0.73) with the DMI index and the analysis results are not sensitive to the choice of the IOD index. Similar to the ENSO, the IOD also modulates the strength of moisture transport over the equatorial Indian ocean [Ashok et al., 2001, Behera and Ratnam, 2018]. A positive IOD condition is found to produce negative IVT anomalies over the eastern equatorial Indian Ocean, north of the equator. We can infer that a positive IOD state would correspond to low-pressure anomalies and higher convective activity over the western Indian Ocean [Saji et al., 1999, Gadgil et al., 2004] which in turn would result in anomalous easterlies (weakened westerlies), reducing the moisture transport across the region. The possible modulation of intraseasonal IVT by the IOD phases was further explored following the same approach as that for ENSO. Seven positive and seven negative IOD years were identified during 1979-2018 (Table 1). Frequency analysis brings out a similar preference for intraseasonal IVT activity as the ENSO phases (Figure 12d). When IOD is positive the intraseasonal IVT is preferentially more active over the subcontinent (36%), compared to equatorial Indian Ocean (19%). And when IOD is negative,

409 the intraseasonal IVT is preferentially more active over the equatorial Indian Ocean (36%), as
410 opposed to the continental domain (16%). However, unlike the ENSO, the direct impact of
411 IOD on monsoon precipitation, independent of ENSO state, is something that is not well
412 understood. Nevertheless, analysis of intraseasonal IVT during positive and negative IOD
413 phases brings out a similar phase preference like those for El Niño and La Niña, which
414 indicate that negative IOD years may be more favorable for intraseasonal convective activity
415 over the subcontinent. While it is difficult to draw out a clearer cause-effect relationship at
416 this stage without targeted largescale modeling experiments, the analysis brings out how the
417 large-scale climate factors like the ENSO and the IOD can modulate the mean IVT and
418 precipitation over the monsoon domain by modulating the intraseasonal modes of IVT and
419 convection.

420 **4. Summary and Conclusions**

421 In this study, we have extracted the subseasonal modes of IVT variability over the
422 ISM domain and examined their characteristics and form of relationship with the ISM
423 precipitation modes during boreal summer seasons from 1979-2018. The subseasonal IVT
424 modes over the ISM domain were extracted by performing an EOF analysis of daily IVT
425 anomalies. The first two EOF modes capture the two phases of the intraseasonal (20-60 days)
426 IVT variability, the third mode captures the quasi-biweekly scale IVT variability (10-20
427 days) and the fourth mode captures the synoptic scale (3-10 days) IVT variability. Among the
428 three subseasonal modes, the intraseasonal scale exhibit the largest amplitude and it is mostly
429 active over the AS, BoB, and adjoining Indian landmass. Whereas, the quasi-biweekly and
430 synoptic-scale IVT modes are prominently active over the BoB, head bay and the foothills of
431 Himalayas. Synoptic scale IVT was found to be the most dominant mode over the Indo-
432 Gangetic plains, suggesting the role of monsoon low-pressure systems in transporting
433 moisture across the region.

Lead-lag correlation analysis of precipitation anomalies with respect to the PCs from IVT EOF analysis, was used to bring out the relationship between IVT and precipitation in the three subseasonal timescales. An interesting finding is that in the intraseasonal, quasi-biweekly and synoptic timescales, the IVT variability lags the precipitation variability, which indicates that the subseasonal variations in IVT over the ISM domain might be driven by the subseasonal variations in precipitation and the circulation responses to the changes in diabatic heating. The lead-lag correlation maps bring out the large-scale tilted structure of the MISOs and their north-south excursion in the intraseasonal time scale and north-westward propagation of disturbances over the ISM domain in the synoptic and quasi biweekly timescales. The northwestward propagation extends from the western Pacific in the case of quasi-biweekly mode, while for the synoptic-scale the propagation is limited to the Indian Ocean domain. This is consistent with the fact that the 10-20 day variability of monsoon precipitation is modulated by northwestward propagating disturbances from the western Pacific and the main synoptic scale features of monsoons are the lows and depressions, which forms over the BoB and propagate towards the core monsoon zone.

Further exploring the predictive potential associated with the subseasonal IVT modes, we examined the influence of the intraseasonal IVT mode in modulating the IVT variability in quasi-biweekly and synoptic scales. The MISOs in convection are known to impact the shorter timescales by helping in the clustering of synoptic-scale lows and depressions. The phase evolution of intraseasonal IVT over the ISM domain was constructed using PC1 and PC2 and the probability of occurrence of quasi-biweekly and synoptic-scale IVT activity were examined for the six intraseasonal IVT phases. The analysis reveals that a significant fraction (more than 60%) of the quasi-biweekly and synoptic-scale IVT activity occurs mainly when the intraseasonal IVT phase is active over the subcontinent, as compared to when the intraseasonal IVT phase is active over the equatorial Indian Ocean. Since

intraseasonal IVT and precipitation evolution are primarily out of phase with each other, it also means that the modulation of high-frequency IVT variability by the intraseasonal scale mainly happens when intraseasonal convective activity is concentrated over the equatorial Indian Ocean. As the intraseasonal timescale is associated with a larger predictive potential compared to the other two modes, this phase preference may be of critical value for seamless prediction over the ISM domain.

Large-scale factors such as the ENSO and IOD were found to have a negative impact on the mean moisture transport over the ISM domain, as the El Niño and the positive IOD phases are associated with easterly wind anomalies over the equatorial Indian Ocean. The El Niño and positive IOD background conditions were also found to impact the intraseasonal variability of IVT, as these largescale conditions favor intraseasonal IVT active phase over the equatorial Indian ocean, when the intraseasonal convective active phase would be over the subcontinent. La Niña and negative IOD conditions, on the other hand would favor intraseasonal IVT active phase over the equatorial Indian Ocean and convective activity over the subcontinent.

To summarize, our analysis of the subseasonal modes (20-60 day, 10-20 day and 3-10 day) of IVT over the ISM domain indicates that the monsoon diabatic heating in itself is a strong driver of monsoon circulation and moisture transport. Hence, the IVT anomalies in any of the three subseasonal timescales cannot be used as predictors for precipitation variability. Since the seasonal mean monsoon is a cumulative product of precipitation in the subseasonal scales, trends and variability of the seasonal mean monsoon may be considered responsible for the observed trends in moisture transport and not vice versa.

Acknowledgments

NJM acknowledges the Early Career Research grant from SERB-DST, Government of India. DV thanks IISER Pune and MHRD, Government of India for DST INSPIRE undergraduate fellowship. Precipitation data was obtained from the website: https://gpm.nasa.gov/data-access/downloads/trmm ERA-Interim reanalysis data were obtained from the website https://apps.ecmwf.int/datasets/data/interim-full-daily/levtype=sfc/

References

Annamalai, H., & Sperber, K. R., (2005). Regional heat sources and the active and break phases of boreal summer intraseasonal (30–50 day) variability. *Journal of the Atmospheric Sciences*, 62, 2726–2748.

Ashok, K., Guan, Z., & Yamagata, T., (2001). Impact of the Indian Ocean dipole on the relationship between the Indian monsoon rainfall and ENSO. *Geophysical Research Letters*, 28, 4499-4502.

Behera, S. K., & Ratnam, J. V., (2018). Quasi-asymmetric response of the Indian summer monsoon rainfall to opposite phases of the IOD. *Scientific Reports*, 8,123, https://doi.org/10.1038/s41598-017-18396-6.

Bellon, G., and Sobel, A. H., (2008). Instability of the axisymmetric monsoon flow and intraseasonal oscillation. *Journal of Geophysical Res*earch, 113, D07108, doi:10.1029/2007JD009291.

Cadet, D. L., & Greco, S. (1987). Water vapor transport over the Indian Ocean during the 1979 summer monsoon Part. 1: Water vapour fluxes. *Monthly Weather Review*, 115, 653-663.

Cadet, D., & Reverdin, G. (1981). Water Vapour Transport over the Indian Ocean during Summer 1975. *Tellus*, 33, 476-487.

Chatterjee, P., & Goswami, B. N. (2004). Structure, genesis and scale selection of the tropical quasi-biweekly mode. *Quarterly Journal of the Royal Meteorological Society*,130(599),1171–1194.

Chen, T. C., and J. M. Chen (1993). The 10–20-day mode of the 1979 indian monsoon: Its relation with the time variation of monsoon rainfall. *Monthly Weather Review*., 121, 2465–2482.

511 Dee, D. P. et al. (2011). The ERA-Interim reanalysis: configuration and performance of the
512 data assimilation system. *Quarterly Journal of the Royal Meteorological Society*, 137,
513 553–597, https://doi.org/10.1002/qj.828.
514 Dixit, V., & Srinivasan, J. (2011). The role of vertical shear of the meridional winds in the
515 northward propagation of ITCZ. *Geophysical Research Letters*, 38, L08812,
516 doi:10.1029/2010GL046601.
517 Fasullo, J., & Webster, P. J. (2003). A hydrological definition of Indian monsoon onset and
518 withdrawal. *Journal of Climate*,16(3), 200–3211.

519 Findlater, J. (1977). Observational aspects of the low-level cross-equatorial jet stream of
520 the western Indian Ocean. *Pure and Applied Geophysics*,115(5-6), 1251-1262.

521 Gadgil, S., Vinayachandran, P. N., Francis, P. A., & Gadgil, S., (2004). Extremes of the
522 Indian monsoon rainfall, ENSO and equatorial Indian Ocean oscillation. *Geophysical*
523 *Research Letters*, 31, L12213, doi:10.1029/2004GL1019733.
524 Gimeno, L., & Coauthors, (2012). Oceanic and terrestrial sources of continental precipitation.
525 *Review of Geophysics*, 50, RG4003, doi:10.1029/2012RG000389.
526 Gimeno, L., Drumond, A., Nieto, R., Trigo, R. M., & Stohl, A. (2010). On the origin of
527 continental precipitation. *Geophysical Research Letters*, 37, L13804,
528 doi:10.1029/2010GL043712.
529 Goswami, B. N., (2005). South Asian monsoon. Intraseasonal Variability of the Atmosphere–
530 Ocean Climate System. W. K. M. Lau and D. E. Waliser, Eds., Springer, 19–61.
531 Goswami, B. N., & Ajayamohan, R. S. (2001). Intraseasonal oscillations and interannual
532 variability of the Indian summer monsoon. Journal of Climate,14, 1180–1198.
533 Goswami, B. N., Ajayamohan, R. S., Xavier, P. K., & Sengupta, D. (2003). Clustering of
534 synoptic activity by Indian summer monsoon intraseasonal oscillations. *Geophysical*
535 *Research Letters*, 30, 1431, doi:10.1029/2002GL016734.
536 Guan, B., Waliser, D. E., Molotch, N. P., Fetzer, E. J., & Neiman, P. J. (2012). Does the
537 Madden-Julian Oscillation influence wintertime atmospheric rivers and snowpack in
538 the Sierra Nevada? *Monthly Weather Review*, 140, 325-342.
539 Huang, B., et al. (2015). Extended Reconstructed Sea Surface Temperature Version 4
540 (ERSST.v4). Part I: Upgrades and Intercomparisons. *Journal of Climate*, 28, 911-930.

Huffman, G. J., et al. (2007). The TRMM Multi-satellite Precipitation Analysis (TMPA): Quasi-global, multiyear, combined-sensor precipitation estimates at fine scales. *Journal of Hydrometeorology*, 8, 38-55.

Jiang, X., Li, T., & Wang, B., (2004). Structures and Mechanisms of the Northward Propagating Boreal Summer Intraseasonal Oscillation. *Journal of Climate*, 17, 1022-1039.

Jones, C., & Carvalho, L. M. V., (2002). Active and break phases in south American monsoon system. Journal of Climate, 8, 905-914.

Joseph, P. V., & Sijikumar, S., (2004). Intraseasonal variability of the low-level jet stream of the Asian summer monsoon. *Journal of Climate*,17, 1449–1458.

Kikuchi, K., & Wang, B. (2009). Global Perspective of the Quasi-Biweekly Oscillation. *Journal of Climate*, 22,1340–1359.

Konwar, M., Parekh, A., & Goswami, B. N., (2012). Dynamics of east-west asymmetry of Indian summer monsoon rainfall trends in recent decades. *Geophysical Research Letters*, 39, L10708, doi:10.1029/2012GL052018.

Krishnamurti, T. N., & Ardanuy, P. (1980). The 10 to 20-day westward propagating mode and "Breaks in the Monsoons". *Tellus*, 32, 15–26.

Lakshmi, D.D., Satyanarayana, A.N.V. & Chakraborty, A., (2019). Assessment of heavy precipitation events associated with floods due to strong moisture transport during summer monsoon over India. *Journal of Atmospheric and Solar-Terrestrial Phys*ics, 189, pp.123-140.

Lawrence, D. M., & Webster, P. J. (2001). Interannual variations of the intraseasonal oscillation in the south Asian summer monsoon region. *Journal of Climate*, 14 2910–22.

Lau, K-M., & Wu, H. T., (2001). Principal Modes of Rainfall–SST Variability of the Asian Summer Monsoon: A Reassessment of the Monsoon–ENSO Relationship. *Journal of Climate*, 14, 2880-2895.

Levine, R. C., & Turner, A. G. (2012). Dependence of Indian monsoon rainfall on moisture fluxes across the Arabian Sea and the impact of coupled model sea surface temperature biases. *Climate Dynamics*, 38, 2167-2190.

Liebmann, B., Kiladis, G. N., Vera, C. S., Saulo, A. C., & Carvalho, L. M. V., (2004). Subseasonal variations of rainfall in South America in the vicinity of the low-level jet east of the Andes and comparison to those in the South Atlantic convergence zone. Journal of Climate, 17, 3829–3842.

575 Mei, R., Ashfaq, M., Rastogi, D., Leung L. R., & Dominguez, F. (2015). Dominating controls
576 for wetter south Asian summer monsoon in the twenty-first century. *Journal Climate*,
577 28, 3400–3419.
578 Murakami, T., Nakazawa, T., & He, T. (1984). On the 40–50 day oscillation during the 1979
579 Northern Hemisphere summer: Part II: Heat and moisture budget. *Journal of the*
580 *Meteorological Society of Japan*,62, 469–484.
581 Ordóñez, P., Ribera, P., Gallego, D., & Peña-Ortiz, C., (2013). Influence of Madden–Julian
582 oscillation on water budget transported by the Somali low-level jet and the associated
583 Indian summer monsoon rainfall. *Water Resources Research*, 49, 6474–6485,
584 doi:10.1002/wrcr.20515.
585 Ortega, S., Webster, P. J., Toma, V., Chang, H. R., (2016). Quasi-biweekly oscillations of the
586 South Asian monsoon and its co-evolution in the upper and lower troposphere. Climate
587 Dynamics, DOI 10.1007/s00382-016-3503-y.
588 Pathak, A., Ghosh, S., Martinez, J. A., Dominguez, F., & Kumar, P. (2017a). Role of Oceanic
589 and land moisture source and transport in the seasonal and interannual variability of
590 summer monsoon in India. *Journal of Climate*, 30, 1839-1859.
591 Pathak, A., Ghosh, S., Kumar, P., Murtugudde, R. (2017b) Role of oceanic and terrestrial
592 atmospheric moisture sources in intraseasonal variability of Indian summer monsoon
593 rainfall. *Nature Scientific Reports*, 7:12729.
594 Patil, C., Prabhakran, T., Sinha Ray, K. C., Anandkumar, K. (2019). Revisiting moisture
595 transport during the Indian summer monsoon using the moisture river concept. *Pure*
596 *and Applied Geophysics*, 176, 5107-5123.
597 Praveen, V., Sandeep, S., & Ajayamohan, R. S. (2015). On the relationship between mean
598 monsoon precipitation and low pressure systems in climate model simulations. *Journal*
599 *of Climate*, 28, 5305-5324.
600 Ratna, S. B., Cherchi, A., Joseph, P. V., Behera, S. K., Abhish B., & Masina, S. (2016).
601 Moisture variability over the Indo-Pacific region and its influence on the Indian
602 summer monsoon rainfall. *Climate Dynamics*, 46, 949-965.
603 Sahana, A. S., Pathak, A., Roxy, M. K., & Ghosh, S., (2019). Understanding the role of
604 moisture transport on the dry bias in indian monsoon simulations by CFSv2. *Climate*
605 *Dynamics*, https://doi.org/10.1007/s00382-018-4154-.
606 Saji, N. H., Goswami, B. N., Vinayachandran, P. N., & Yamagata, T., (1999). A dipole mode
607 in the tropical Indian Ocean. *Nature*, 401, 360 – 363.

Sandeep, S., & Ajayamohan, R. S. (2015). Poleward shift in Indian summer monsoon low level jetstream under global warming. *Climate Dynamics*, 45, 337–351.

Suhas, E., Neena, J. M., & Goswami, B. N., (2012). Interannual variability of Indian summer monsoon arising from interactions between seasonal mean and intraseasonal oscillations. *Journal of the Atmospheric Sciences*, 69,1761-1774.

Suhas, E., Neena, J. M., & Goswami, B. N., (2013). An Indian monsoon intraseasonal (MISO) index for real-time monitoring and forecast verification. *Climate Dynamics*, 40, 2605–2616 DOI 10.1007/s00382-012-1462-5.

Varikoden, H., Revadekar, J. V., Kuttipurathu, J., & Babu, C. A., (2018). Contrasting trends in southwest monsoon rainfall over the Western Ghats region of India. *Climate Dynamics*, https://doi.org/10.1007/s00382-018-4397-7.

Waliser, D. E., & Guan, B. (2017). Extreme winds and precipitation during landfall of atmospheric rivers. *Nature Geoscience*, 10, 179-183.

Webster, P. J., & Fasullo, J., (2003). Dynamic theory of monsoons. *Encyclopaedia of Atmospheric Sciences*, Academic Press, 1370-1386.

Webster, P. J., & Yang, S., (1992). Monsoon and ENSO: A selectively interactive systems. *Quarterly Journal of the Royal Meteorological Society*, 118, 877-926.

Webster, P. J., Magaña, V. O., Palmer, T. N., Shukla, J., Tomas, R. A., Yanai, M., & Yasunari, T. (1998). Monsoons: processes, predictability, and the prospects for prediction. *Journal of Geophysical Research*, 103,14451.

Yoon, J-H., & Chen T-C., (2005). Water vapor budget of the Indian monsoon depression. *Tellus*, 57, 770-782.

El Niño	La Niña	Positive IOD	Negative IOD
1982	1985	1982	1984
1987	1988	1994	1985
1991	1998	1997	1992
1997	2000	2003	1996
2002	2008	2006	1998
2004	2010	2008	2010
2009	2016	2015	2016
2012			
2015			

Table 1. List of El Niño, La Niña, positive and negative IOD years for the period 1979-2018.

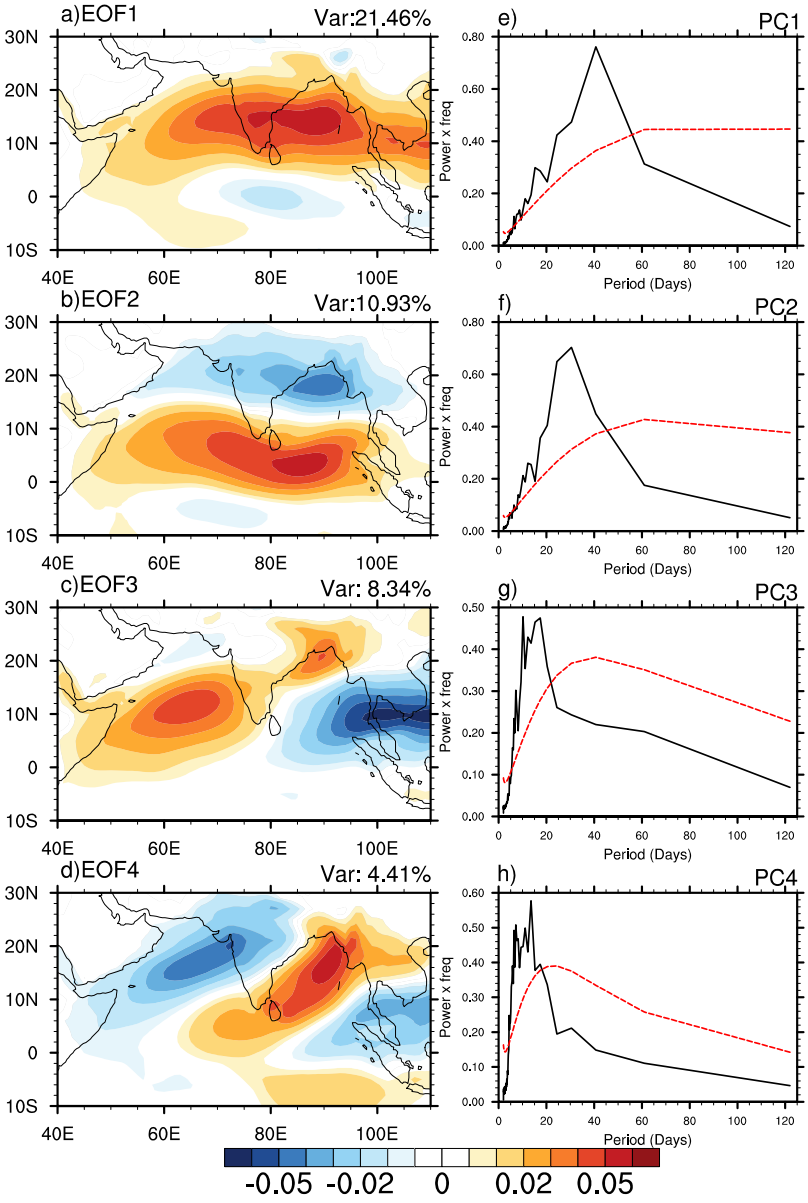

Figure 1. a) to d) First four empirical orthogonal function (EOF) modes of daily integrated water vapor transport (IVT) anomalies calculated for boreal summer seasons (June to September) from 1979-2018. Fractional variance explained by each mode is shown on the upper righthand side of the plots. e) to h) Power spectra of the principle components (PC) correspond to first four EOF modes (Black solid line). The red dashed line represents the red-background spectra.

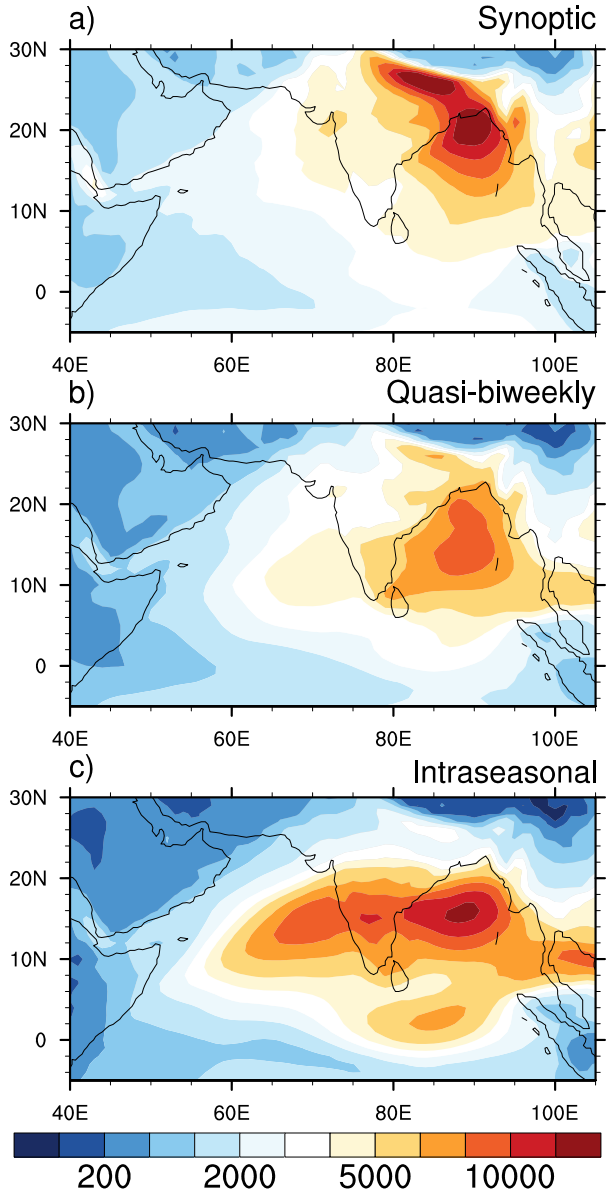

Figure 2. a) synoptic (3-10 days), b) quasi-biweekly (10-20 days), and c) intraseasonal scale (20-60 days) variance of IVT for boreal summer seasons from 1979-2018. Variances are estimated using bandpass filtered daily IVT data.

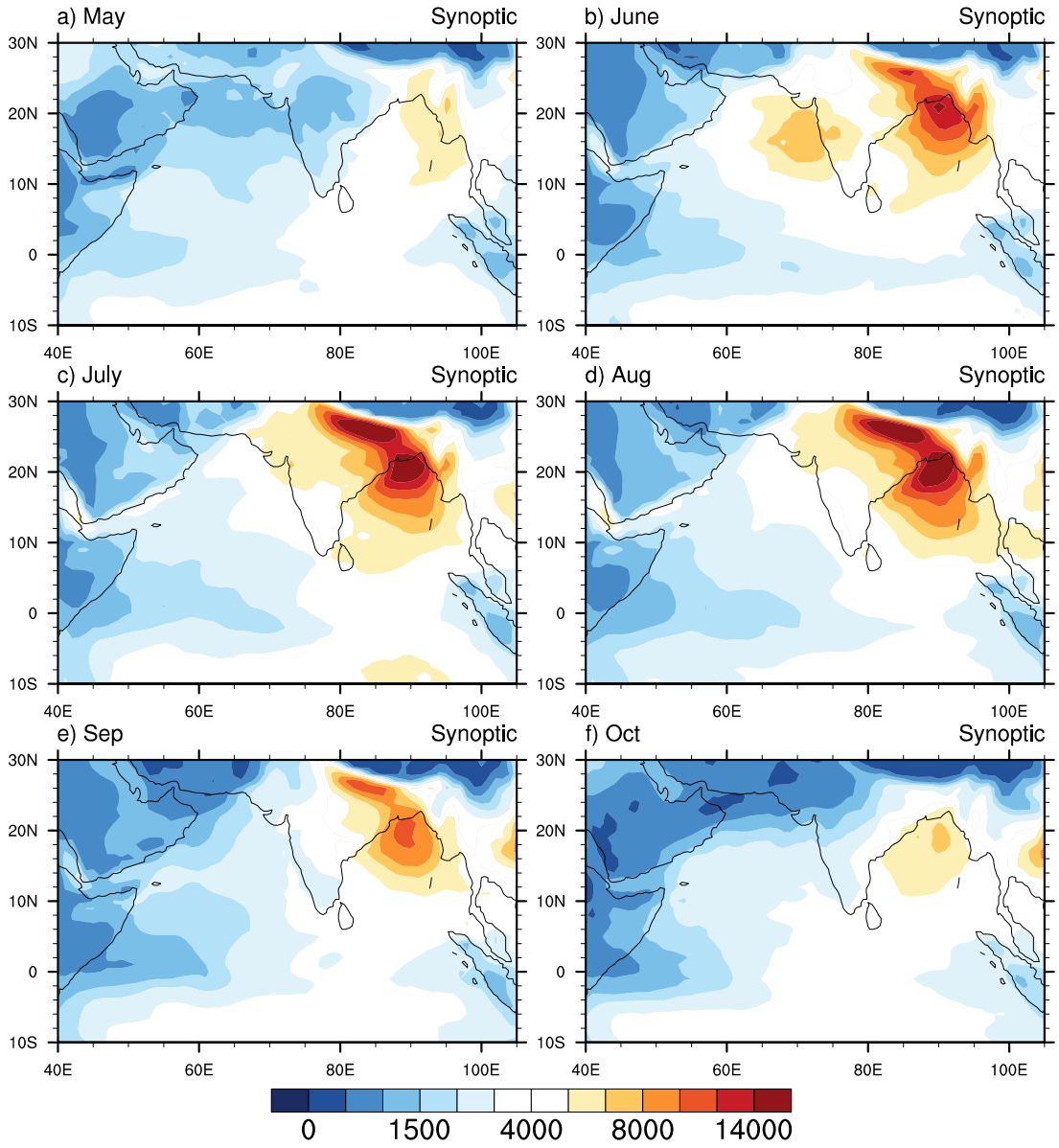

Figure 3. Synoptic-scale IVT variance during May to October months for the period 1979-2018.

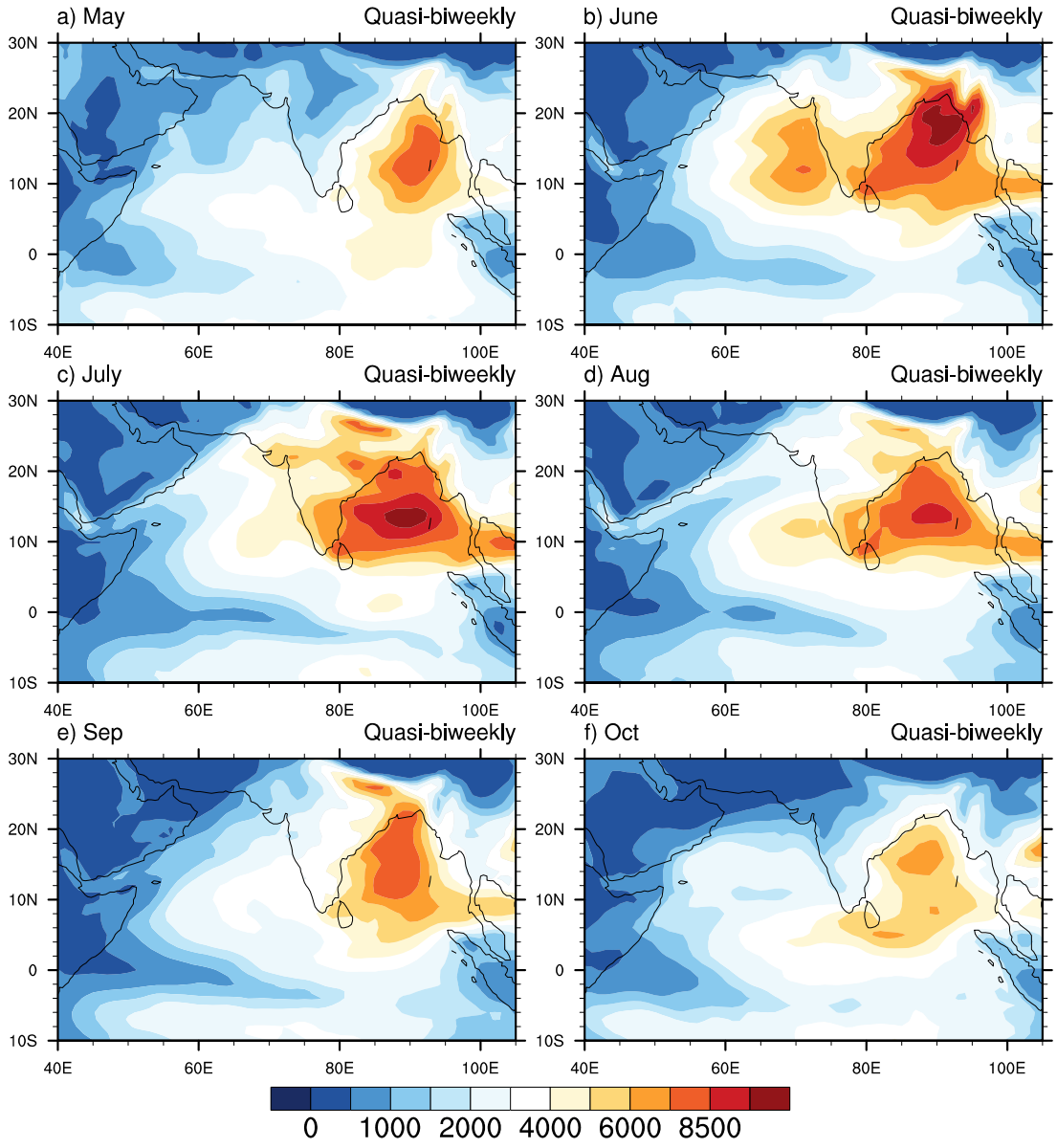

Figure 4. Quasi-biweekly scale IVT variance during May to October months for the period 1979-2018.

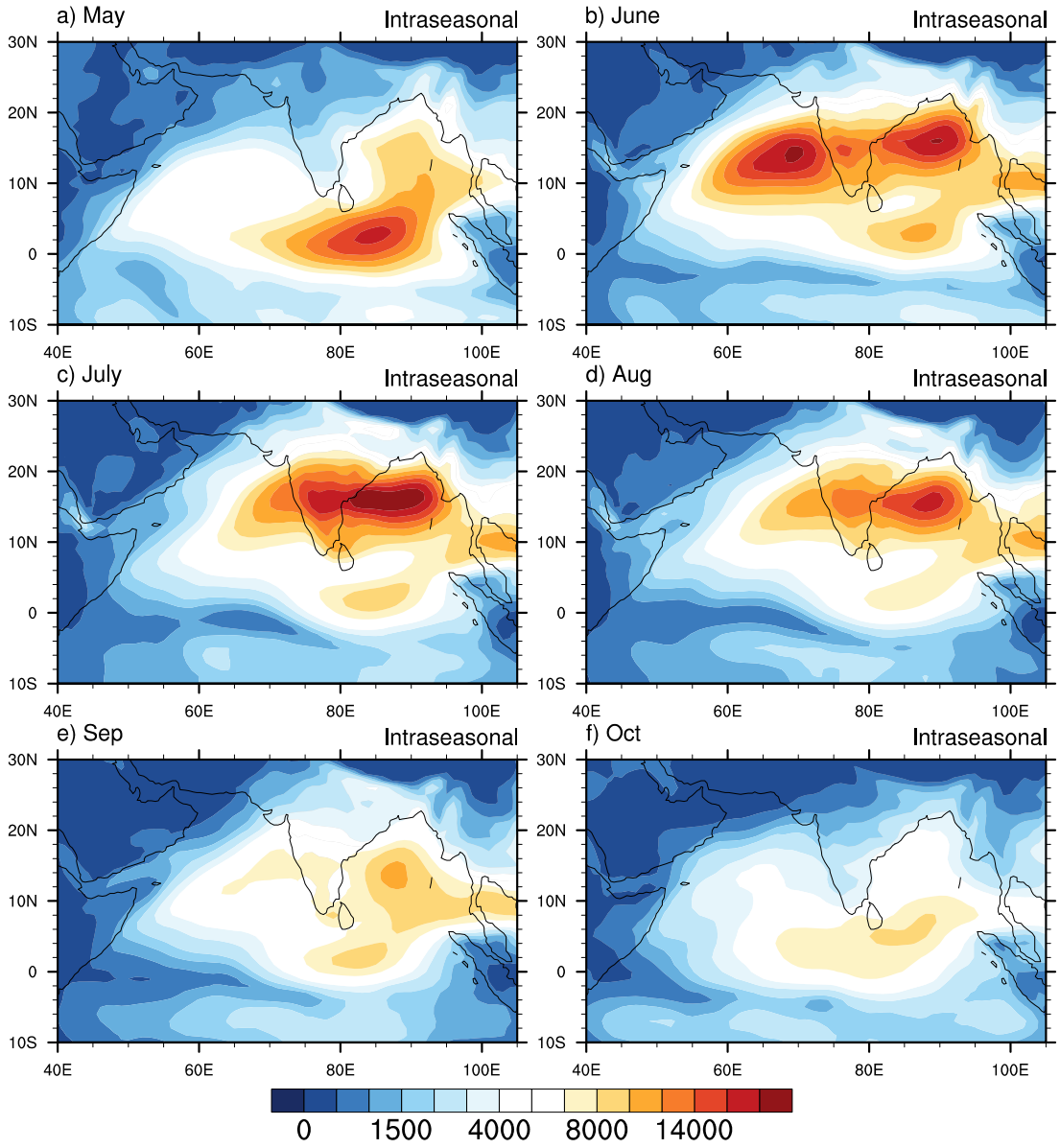

Figure 5. Intraseasonal scale IVT variance during May to October months for the period 1979-2018.

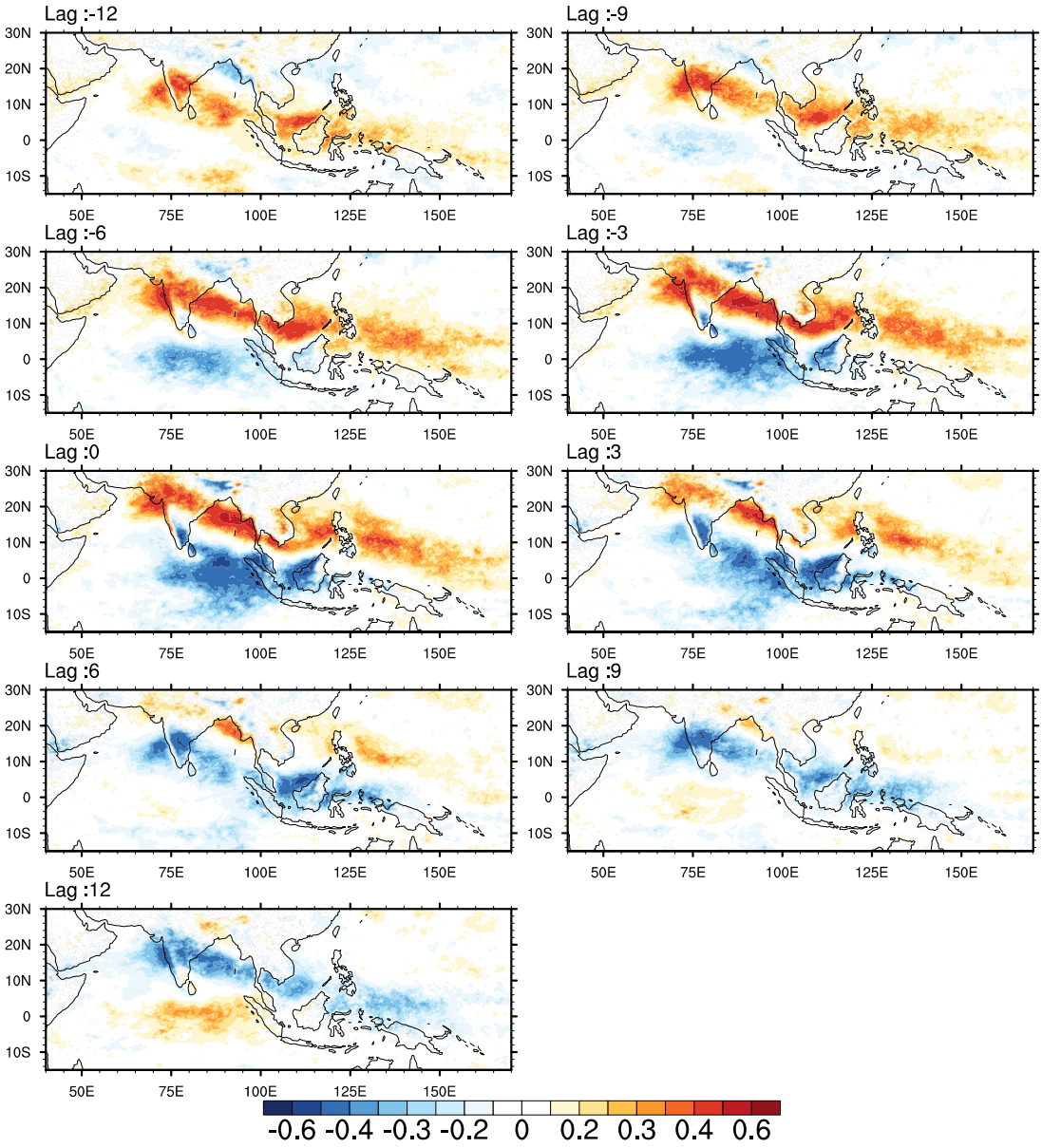

Figure 6. Lead-lag correlation of 25-60 day filtered precipitation anomalies with the intraseasonal IVT index (PC1) for boreal summer seasons from 1979-2018. A negative lag represents precipitation leading IVT and a positive lag represents precipitation lagging IVT. Lag days are indicated on the upper left-hand side of each plot.

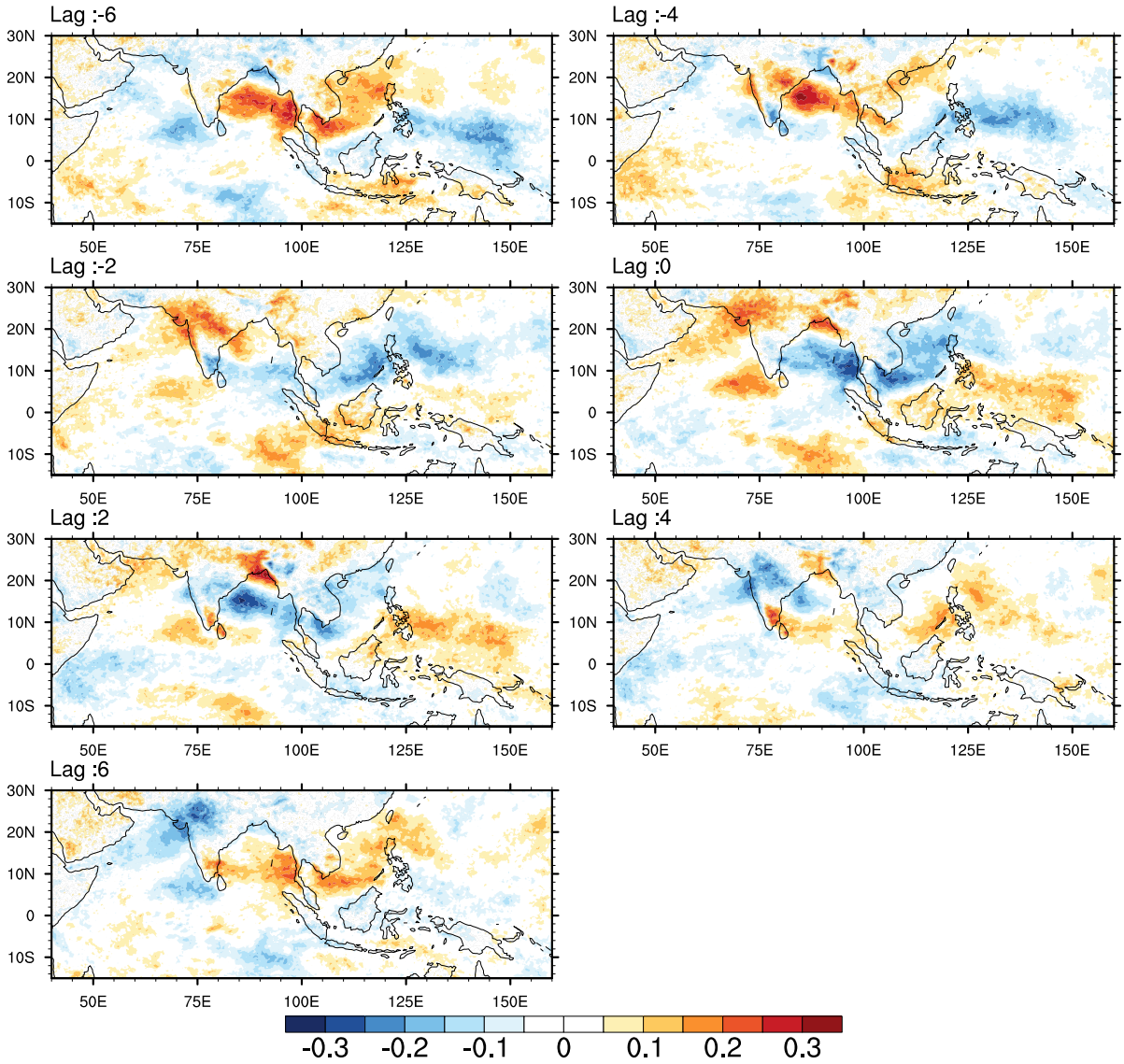

Figure 7. Lead-lag correlation of 10-20 day filtered precipitation anomalies with the quasi biweekly IVT index (PC3) for boreal summer seasons from 1979-2018. A negative lag represents precipitation leading IVT and a positive lag represents precipitation lagging IVT. Lag days are indicated on the upper left-hand side of each plot.

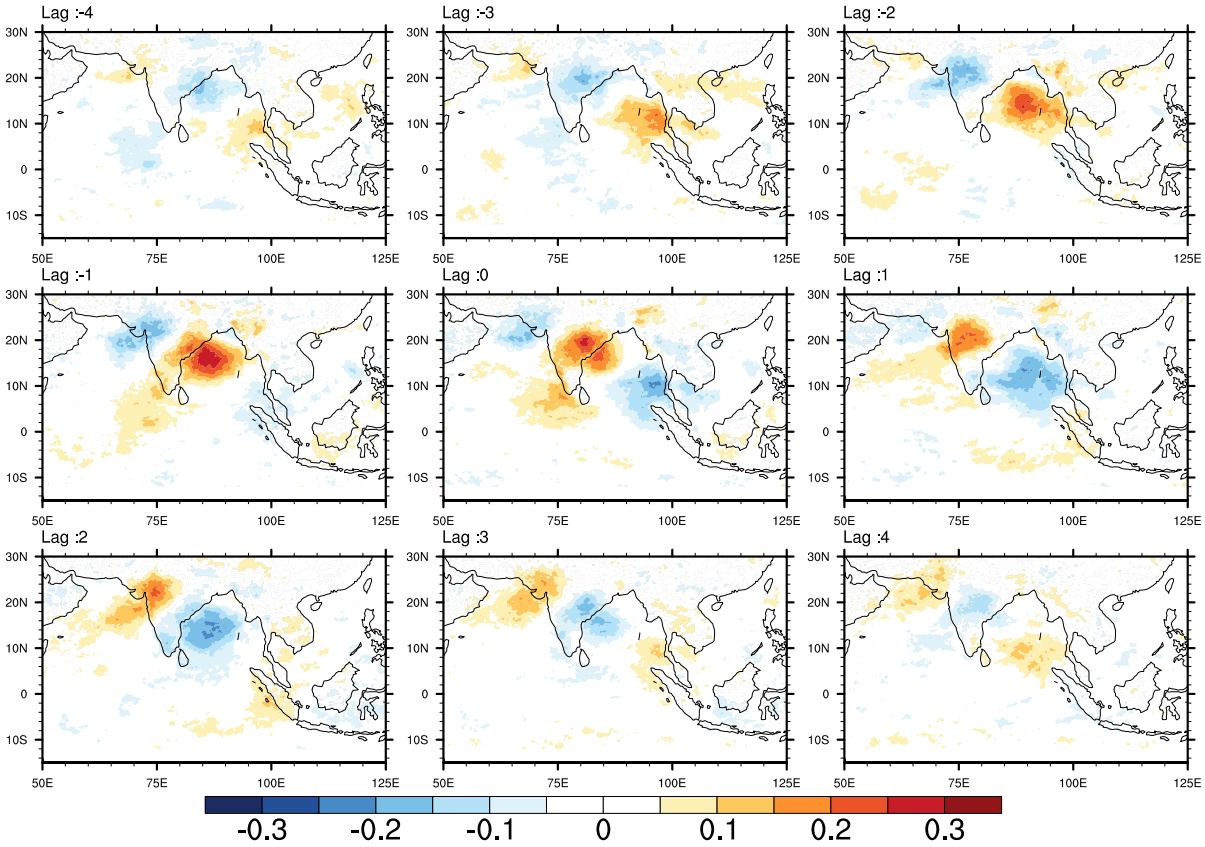

Figure 8. Lead-lag correlation of 3-10 day filtered precipitation anomalies with the synoptic-scale IVT index (PC4) for boreal summer seasons from 1979-2018. A negative lag represents precipitation leading IVT and a positive lag represents precipitation lagging IVT. Lag days are indicated on the upper left-hand side of each plot.

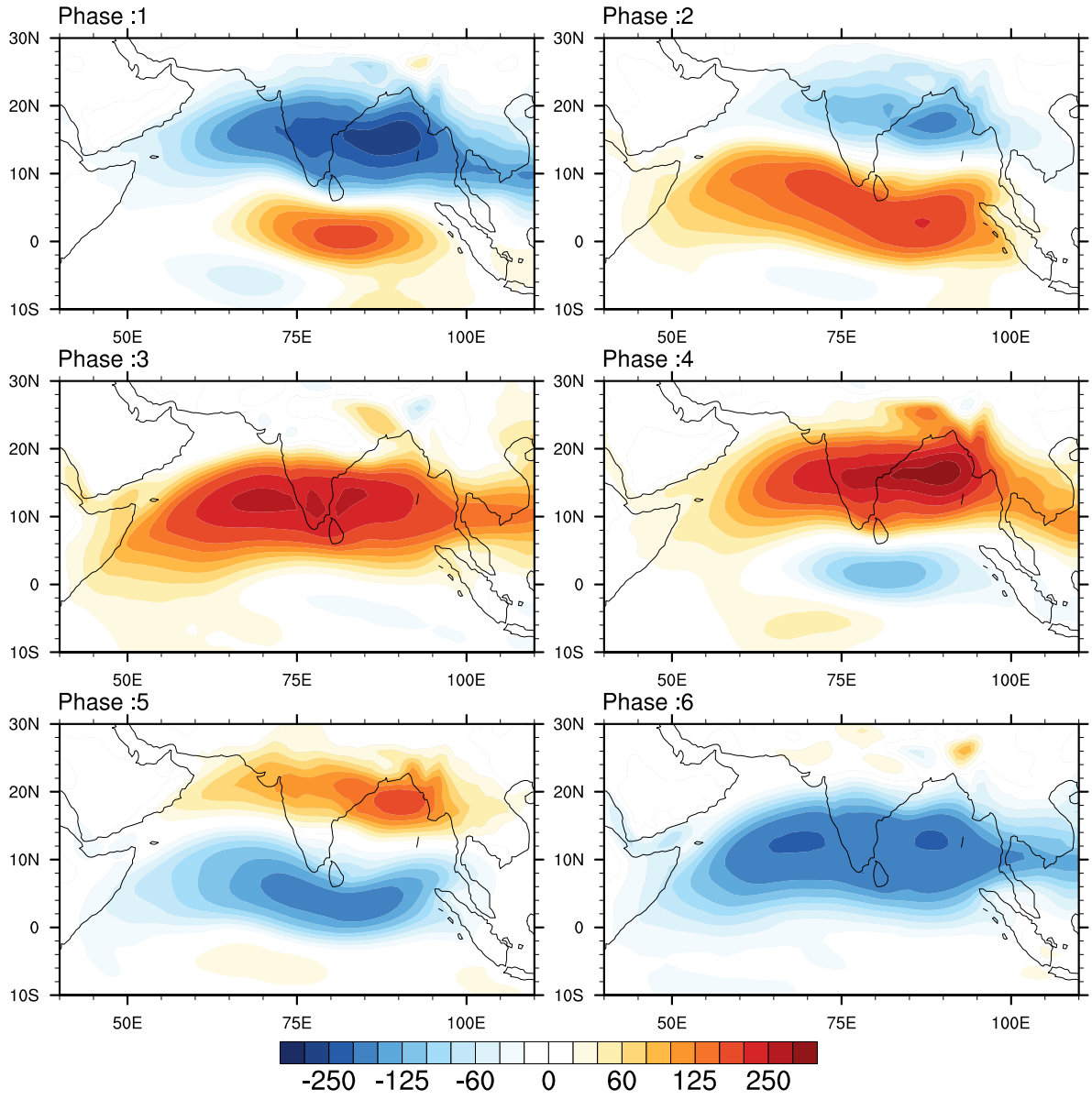

Figure 9. Life cycle composite of daily IVT anomalies over six phases constructed using PC1 and PC2 of the EOF analysis of daily IVT anomalies during boreal summer seasons from 1979-2018.

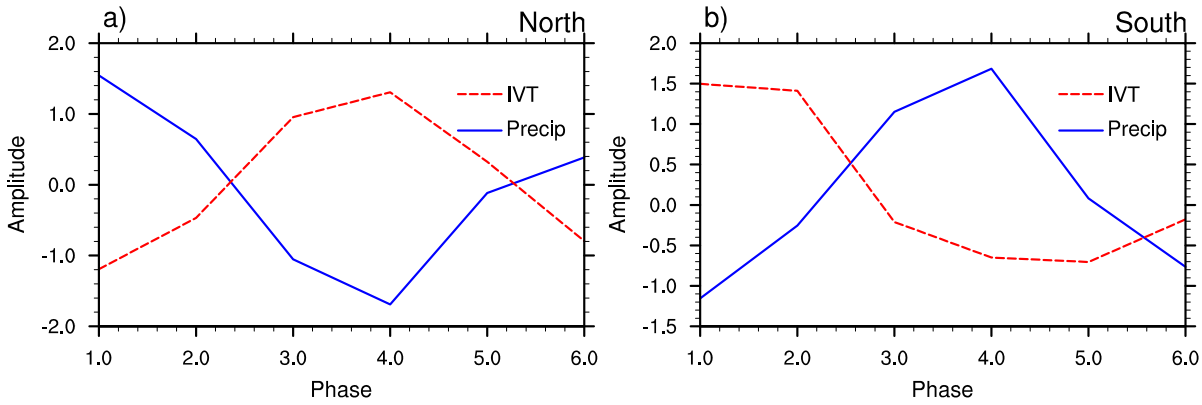

Figure 10. Phase evolution of precipitation and IVT anomalies with respect to the intraseasonal IVT phases. a) To represent the evolution over the subcontinent, the phase composited precipitation anomalies were averaged over 17°-21°N 80°-90°E and the IVT anomalies were averaged over 13°-17°N, 80°-90°E. b) To represent the evolution over the equatorial Indian ocean, the phase composited precipitation and IVT anomalies were averaged over 5°S-0, 80°-90°E.

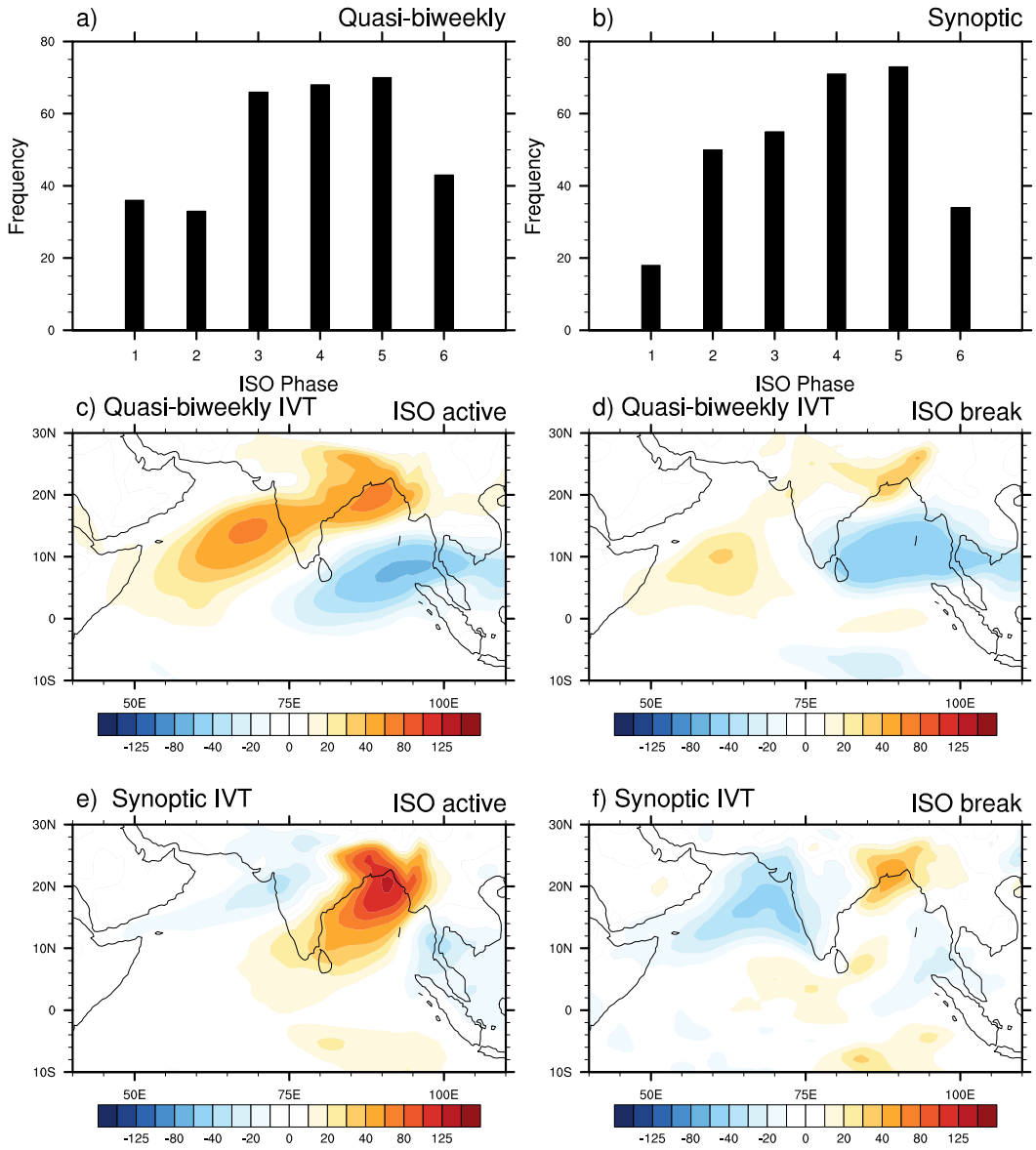

Figure 11. a) Quasi-biweekly IVT activity during the six intraseasonal IVT phases measured as the number of days when the quasi biweekly scale IVT mode is active (normalized PC3 >1), b) Synoptic scale IVT activity during the six intraseasonal IVT phases measured as the number of days when the synoptic-scale IVT mode is active (normalized PC4 >1)

Daily IVT anomalies composited for days when the quasi biweekly scale IVT mode is active (PC3 >1) and the intraseasonal IVT phase is active c) over the subcontinent (Phases 3, 4, and 5) and d) over equatorial Indian ocean (Phases 6, 1, and 2). e) and f) similar to c) and d) but when the synoptic-scale IVT mode is active (PC4 >1).

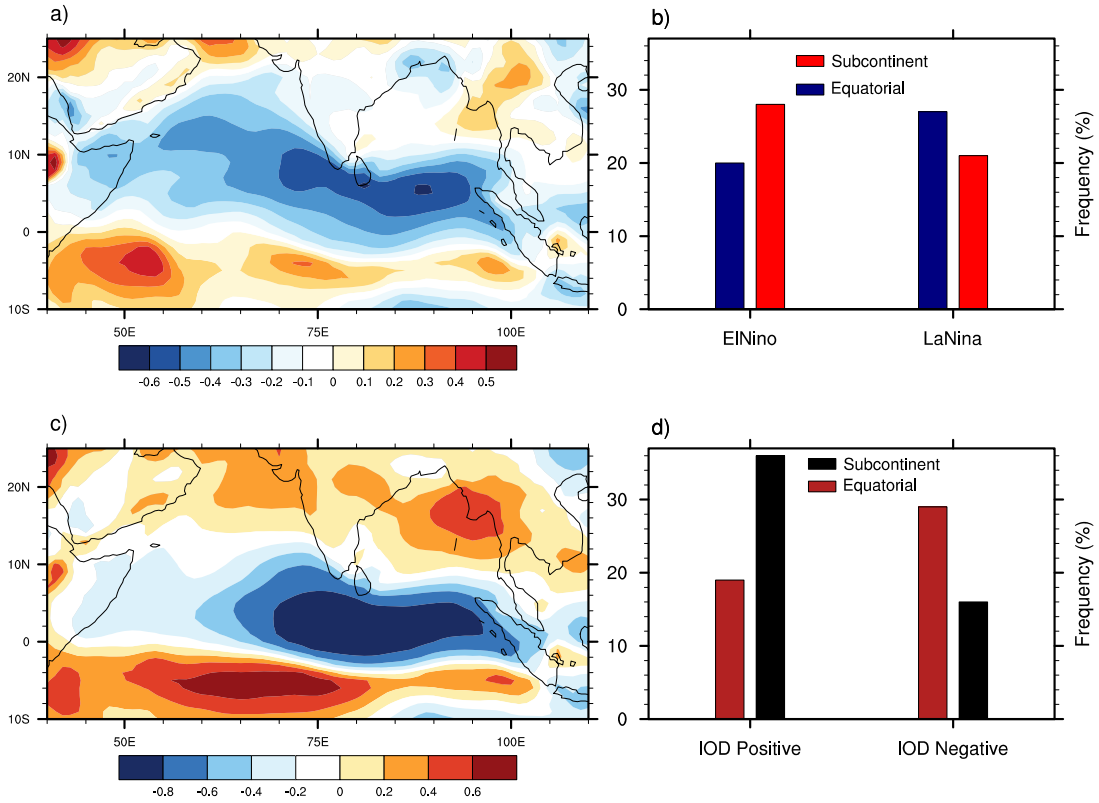

Figure 12. Boreal summer seasonal mean IVT correlated with the a) NINO 3.4 index c) EQUINOO index during 1979-2018. b) Percentage of days when the intraseasonal IVT active phase is over the subcontinent (Phases 3, 4, and 5) and over equatorial Indian ocean (Phases 6, 1,2), for El Niño and La Niña years. d) same as b) but for positive and negative IOD years.